American Laboratory

RECENT DEVELOPMENTS IN

High-field nmr spectroscopy of biological systems

By E. Oldfield, H.S. Gutowsky, R.E. Jacobs, S.Y. Kang, M.D. Meadows, D.M. Rice, and R.P. Skarjune

IN THE PAST TWO or three years there have been a number of welcome developments in nuclear magnetic resonance studies of biological systems, especially those involving high-field investigations of membranes and proteins. In this publication two of these developments of current interest are reported: high resolution ^{13}C Fourier transform studies of protein structure in solution with a sideway-spinning 20-mm sample tube probe and high-field deuterium quadrupole-echo studies of model and biological membrane structure using ^{2}H-labeled lipids.

Two "home-built" Fourier transform nmr spectrometers are used for these high-field studies of membrane and protein structure in the authors' laboratory (*Figure 1*). Their construction is described below.[1,2] These spectrometers operate with "wide-bore" superconductive magnets, each having a room temperature access of about 3 in. Large-bore magnets, although not essential for all nmr investigations of biological systems, facilitate the study of single-carbon atom sites in proteins by enabling relatively large sample volumes to be used.

Dr. Oldfield is Assistant Professor of Chemistry, Dr. Gutowsky is Professor of Chemistry, Dr. Jacobs and Dr. Kang are Research Associates, and Mr. Meadows, Mr. Rice, and Mr. Skarjune are Graduate Students, University of Illinois at Urbana-Champaign. *This research was supported by the National Science Foundation (Grants PCM 76-01491, CHE 77-04585), by the National Institutes of Health (Grant HL-19481), by the American Heart Association with funds provided in part by the Illinois Heart Association (Grant 77-1004), by the Illinois Heart Association (Grant N-6), and by the Alfred P. Sloan Foundation.*

Figure 1 *High-field nmr spectrometers used to obtain data. The 5.2-tesla deuterium instrument (34 MHz), left, and the 3.5-tesla ^{13}C instrument (37.7 MHz), right. The superconducting solenoids are not shown.*

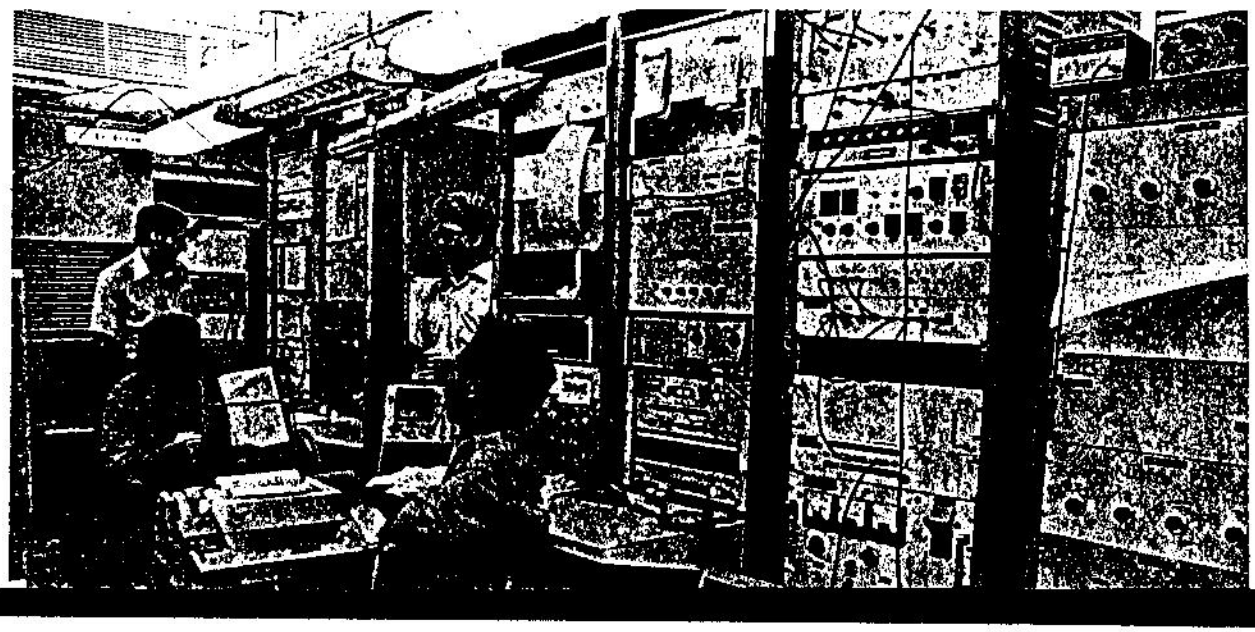

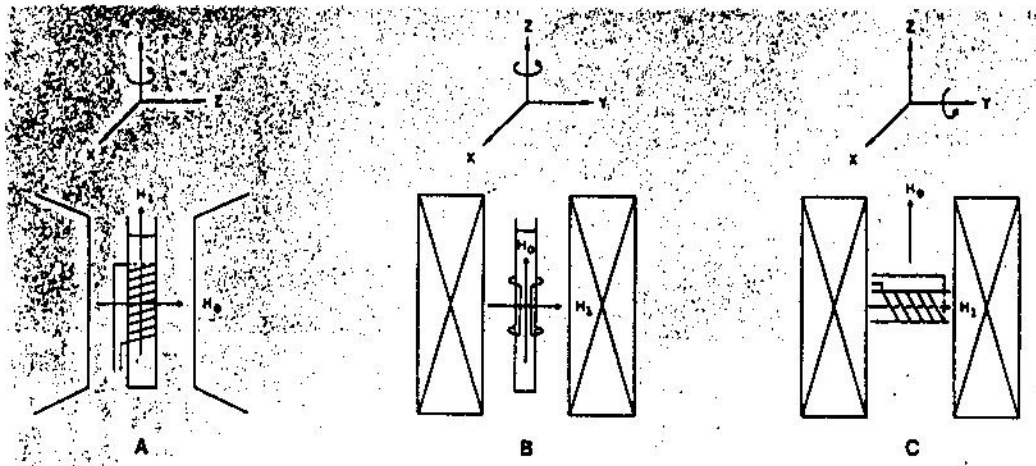

Figure 2 *The three principal magnet and rf coil configurations used in nmr spectrometers. a) Conventional horizontal electromagnet with cylindrical solenoid rf coil. Sample spins about y-axis. b) Vertical solenoid magnet with Helmholtz rf coil. Sample spins about z-axis. c) Vertical solenoid magnet with cylindrical solenoid rf coil. Sample spins about y-axis. The large rectangles in b and c represent vertical sections through the solenoid magnet. The 20-mm sideways-spinning tube (SST) probe used to obtain natural abundance ^{13}C spectra uses the configuration shown in c.*

In addition, wide-bore magnets can accommodate complex probe assemblies: for example, those used in variable-temperature "magic-angle" proton-decoupled carbon-13 experiments.

There are two main reasons why the study of proteins in solution by ^{13}C nmr requires large volumes of sample. First, the solubility of proteins is typically only 20 m*M*; thus, the sample concentration is usually a good deal lower than for small organic molecules. Second, because of their size, the protein molecules have a long rotational correlation time, and therefore, in many instances, only the minimum nuclear Overhauser effect is observed.[3,4] As a result, a larger sample volume is essential to offset the corresponding decreases in sensitivity.

Instrumentation

Results using 20-mm sample tubes were reported in *American Laboratory* some years ago using a spectrometer that operated at 14,000 G with a conventional iron-core electromagnet.[1] In the last three or four years higher-field instruments using superconducting solenoid magnets have been introduced in order to further improve spectrometer sensitivity, although in all instances the gains expected on theoretical grounds[4] have not been realized. The principal reason for the less than optimum performance at high field lies in probe design. In a conventional electromagnet, the dc magnetic field H_0 is horizontal (z-axis) and the orthogonal rf magnetic field is created in a vertical cylindrical solenoid coil. This arrangement is good from an rf standpoint. Moreover, for high resolution nmr the sample is readily spun about the vertical axis (*Figure 2a**).

Now in a superconducting solenoid (which for most nmr applications consists of a niobium/titanium coil immersed in a bath of liquid helium) the dc magnetic field H_0 is vertical (z-axis) (Figure 2). Thus, the orthogonal rf magnetic field has to be about a horizontal axis, and it is conventionally provided by a pair of Helmholtz or saddle coils. This arrangement permits the sample to be spun about a vertical axis, with ease of removal (and insertion) of the sample from the probe with, for example, a pneumatic ejection system. Unfortunately, it is now well known that Helmholtz-pair coils give decidedly inferior performance to a solenoid geometry. The rf field is inhomogeneous, thus compounding the difficulties of relaxation measurements, but more importantly, coil *Q*'s are lower, which means that transmitter power is wasted and signal-to-noise ratios are decreased. These facts have been known for some time by solid-state workers using superconducting magnets, who, not having the complication of sample spinning (until recently), have used a horizontal solenoid coil (Figure 2b) as the obvious solution. Interestingly, the same commercial superconductivity instrument manufacturers who use Helmholtz coils for solution work also use solenoid coils on their instruments designed for solid-state investigations.

The performance differences between rf solenoid and Helmholtz coils have recently been thoroughly investigated, both experimentally and theoretically, by Hoult and Richards.[7] They conclude that solenoids give about a twofold better signal-to-noise ratio than Helmholtz-coil geometries. The question thus arises of the feasibility of adopting a solenoid-coil geometry for high resolution nmr studies in a superconducting solenoid magnet. It may be significantly more difficult to overcome problems such as dc magnetic field inhomogeneity when the sample lies on its side, since, in general, only relative low order radial correction coils (X^1, Y^1) are provided with solenoid magnets, while axial correction coils are usually available up to Z^1. The choice of these gradients has been tailored to fit the conventional vertically spinning sample tube, where sample length along the z-axis is usually about twice the sample breadth (in the X, Y plane). In addition, for

Figure 3 *A 20-mm sideways-spinning tube probe. The sample rides on air-bearings at each end of the tube. A Helmholtz coil is used for proton-decoupling; the ^{13}C rf solenoid coil is located on the inside of the probe assembly.*

*Reprinted from the *Journal of Magnetic Resonance*, in press, 1978. Copyright 1978 by the Academic Press.

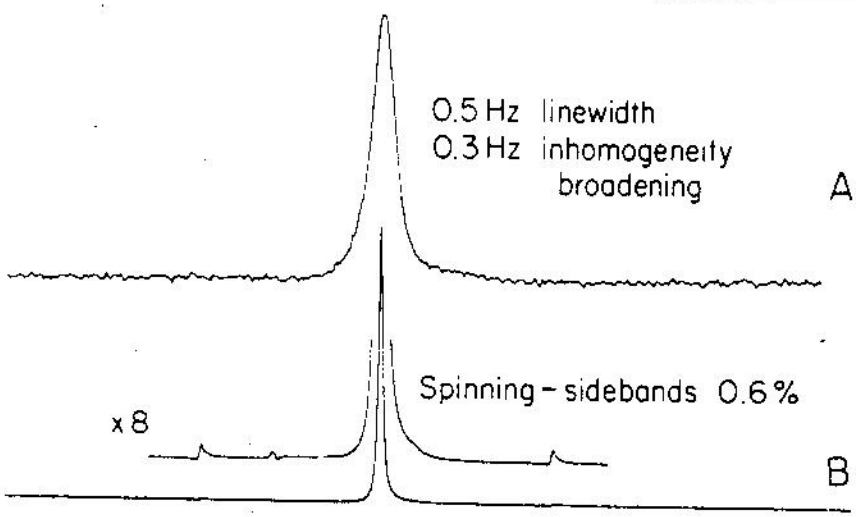

Figure 4 *Line shape and spinning-sideband performance of the sideways-spinning 20-mm tube probe. a) Ethylene glycol spectrum obtained using the Fourier transform method (at 35°, ^{13}C frequency 37.7 MHz, ^{1}H frequency 150.0 MHz, single-frequency decoupling, 5.8-w decoupling power, 21-sec recycle time, 22-μsec 90° pulse width, 100-Hz spectral width, zero acquisition delay time, 2 × 2048 data points, 1 scan, 1000-Hz 4-pole Butterworth low-pass filters, no line broadening). The sample volume was 6.5 ml and the spinning rate about 70 revisec. An inhomogeneity broadening of about 0.3 Hz is inferred. b) As in (a) except 128 scans, 1000-Hz spectral width, 1.5-Hz line broadening. Spinning sidebands are about 0.6% main peak intensity.*[1]

good high resolution spectra, we must be able to maintain stable horizontal sample spinning, with no degradation of magnetic field homogeneity due to formation of "bubbles."

We have recently constructed sideways-spinning sample probes for 20- and 30-mm sample tubes and find with our probe and magnet combination that none of the above considerations causes any resolution problems for carbon-13 studies of macromolecules. *Figure 3** is a photograph of the 20-mm tube sideways-spinning probe[1] operated at about 37.7 MHz in a wide-bore 35.2 kG superconductive magnet (Nicolet Nalorac Corp.). This magnet has a helium bore of 5.0 in., a room temperature bore of 4.0 in., and a room temperature access of about 3.0 in. when equipped with room temperature shim coils (Z, Z^2, Z^3, Z^4, X, Y, XZ, YZ, X^2-Y^2, XY, X^3, and Y^3 gradients).

Figure 4a shows a typical carbon-13 nmr line shape obtained from a sample of ethylene glycol in the 20-mm SST probe, which contains about 6.5 ml of sample (both sample and radiofrequency coil length are 1 in.). The observed line width is about 0.5$_0$ Hz, of which about 0.2$_0$ Hz is natural line width. Inhomogeneity broadening of about 0.3 Hz thus is obtained, fairly routinely. Since our probe was developed to facilitate studies of single-carbon

*Figures 3 and 5 are reprinted from the *Journal of Magnetic Resonance*, in press, 1978. Copyright 1978 by the Academic Press.

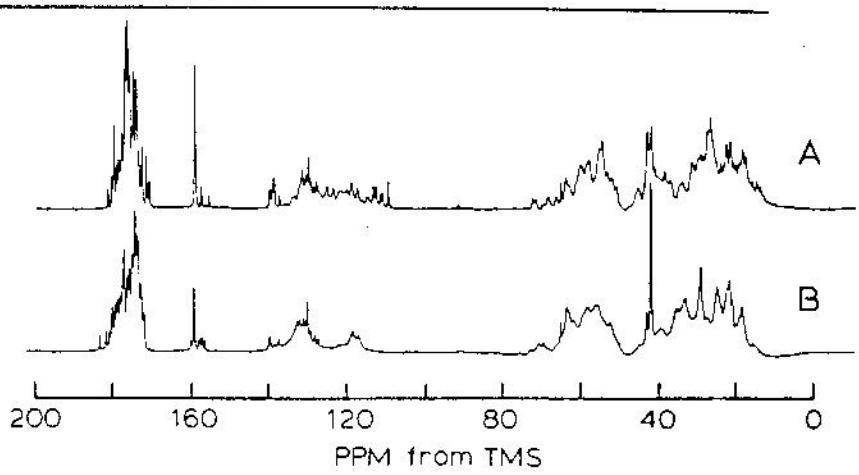

Figure 5 *Proton-decoupled natural-abundance ^{13}C Fourier transform nmr spectra obtained using a sideways-spinning 20-mm tube probe with 6.5 ml of sample. a) Hen egg-white lysozyme (EC 3.2.1.17, Sigma Chemical Co., Type I, further purified by chromatography on diethylaminoethyl-Sephadex) in H_2O (19 mM, pH 3.3, about 35°, ^{13}C frequency 37.7 MHz, ^1H frequency 150.0 MHz, noise modulation of 1369-Hz bandwidth, 4.4-w decoupling power, 3.0-sec recycle time, 22-μsec (90°) pulse width, 8547-Hz spectral width, 350-μsec acquisition delay time, 2 × 8192 data points, 15216 scans, 5000-Hz 4-pole Butterworth low-pass filters, 1.5-Hz line broadening). b) Bovine pancreatic ribonuclease A (EC 2.7.7.16, Sigma Chemical Co., Type IIA) in H_2O (17 mM, pH 4.3, 23554 scans, all other conditions as in*

atom sites in proteins, this resolution is more than adequate. In addition, spinning side bands are typically 0.5–1.0% (Figure 4*b*). Air bubbles or sample vortexing does not cause shimming problems since an "air-tube" forms along the spinning axis of the sample. Homogeneity changes are very small because of this symmetric arrangement.

The sensitivity of the probe is paramount in importance. We obtain a root-mean-square signal-to-noise ratio of about 230:1 with a single 90° pulse on a 6.5-ml sample of neat dioxane, when using quadrature phase detection and utilizing a 1.5-Hz line broadening (due to exponential multiplication of the free-induction decay). This is comparable to that obtained by commercial systems operating in the 3.5–4.2 tesla field range with Helmholtz rf coil probes, but which use up to twice our sample volume. For microsamples and for very high frequency applications—for example, in a 360-MHz (8.5-tesla) proton instrument—it is clear that the signal-to-noise ratio gains of the SST probe will be even more impressive due to the increased difficulties at these high frequencies of winding Helmholtz coils for either micro or very large samples.

Our 20-mm SST probe was designed principally to study protein structure using natural-abundance carbon-13 Fourier transform nmr spectroscopy. *Figure 5* shows typical ^{13}C signal-to-noise ratios achieved when using about 6.5 ml of aqueous hen egg-white lysozyme (EC 3.2.1.17) and bovine pan-

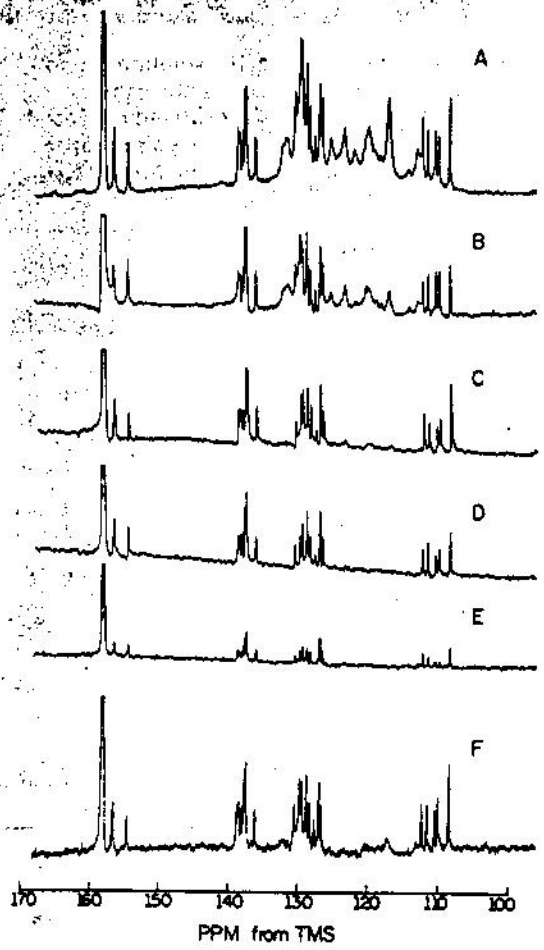

Figure 6 *Proton-decoupled natural-abundance ^{13}C normal and spin-echo Fourier transform nmr spectra of 6.5 ml aqueous solution of hen egg-white lysozyme (EC 3.2.1.17) obtained using a sideways-spinning 20-mm tube probe. a) Hen egg-white lysozyme (described in Figure 5a) in H_2O (19 mM, pH 2.8, about 37°, ^{13}C frequency 37.7 MHz, ^1H frequency 150.0 MHz, noise-modulation of 1800-Hz bandwidth, 5.6-w decoupling power, 6.0-sec recycle time, 22-μsec (90°) pulse width, 8547-Hz spectral width, 350-μsec acquisition delay time, 2 × 8192 data points, 12,000 scans, 5000-Hz 4-pole Butterworth low-pass filters, 1.5-Hz line broadening). b–e) As in (a) but spin-echo spectra obtained using the Carr-Purcell method with the following τ values and delay times: b) 6 msec, c) 20 msec, d) 40 msec, e) 150 msec, and f) spin-lock FT spectrum with 40-msec spin-lock pulse.*[9]

creatic ribonuclease A (EC 2.7.7.16). Clearly, instrumentation improvements have brought very welcome signal-to-noise ratio increases in the six years following the first report of resolved single-carbon atom sites in proteins in *American Laboratory*.[4] The improved sensitivity of the SST probe facilitates, for example, relaxation studies on single-carbon atom sites in proteins.

Figure 6 shows the results of a two-pulse, Carr-Purcell experiment[9] in the aromatic region of an aqueous solution of hen egg-white lysozyme.[9] In the normal (unrelaxed) ^{13}C Fourier transform spectra (Figure 6*a*), two types of resonance may be distinguished[10]: broad resonances, which arise from protonated (methine) carbon atoms, and relatively narrow resonances, which arise from nonprotonated aromatic carbons.[10] The very short transverse relaxation times of the methine carbon atom resonances, due to efficient carbon-hydrogen dipolar relaxation, means that at long τ values there is no refocusing of magnetization from these sites. However, nonprotonated carbon atoms have relatively long spin-spin relaxation times, due to weak dipolar interactions and chemical shift anisotropy,[9] so that in a partially T_2– relaxed spectrum it is possible to

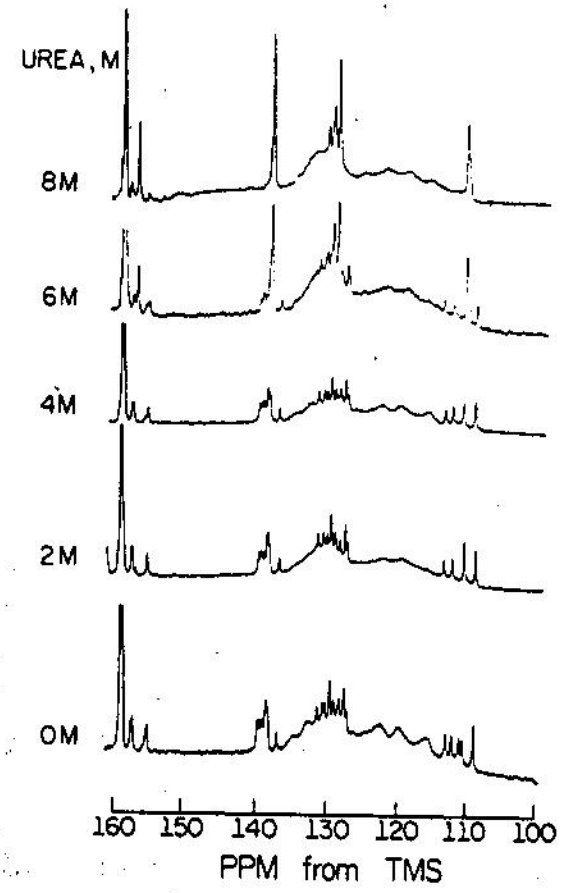

Figure 7, right. *Natural-abundance ^{13}C Fourier transform nmr spectra of hen egg-white lysozyme (EC 3.2.1.17), obtained under conditions of weak proton decoupling, in the presence of various mole fractions of the denaturing agent urea. The spectral region shown contains aromatic and C^{ζ} of arginine resonances.*[34]

completely eliminate all contributions from methine aromatic carbon atom sites, as shown for example in Figure 6*d*. The method is thus an alternative to convolution-difference spectroscopy.[11]

Carbon-13 studies of protein denaturation

Using the 20-mm SST probe we are investigating the denaturation of proteins by reagents such as urea, guanidinium chloride, and 2-bromoethanol. High signal-to-noise ratios are of course essential in order to detect possible intermediate partially unfolded species present only in low concentrations. *Figure 7* shows representative results from a denaturation study of hen egg-white lysozyme with urea as the denaturant. It is seen that as urea is added, a new, simpler ^{13}C spectrum grows, while the more complex spectrum of the native protein disappears. For example, the group of 5 lines (6 carbons) near 110 ppm in the bottom spectrum is replaced by a single line at the top. No evidence to date has been found for intermediate species by ^{13}C nmr, and the process clearly seems to be a conversion between two states.

Nonetheless, prior to denaturation there are several sizable chemical shift changes, interestingly, in residues that are known to be in or near the active site of the enzyme (Trp 62 and 108). An understanding of the significance of these chemical shift changes probably will require a much better knowledge of the mechanisms governing the chemical shift nonequivalences observed in the native protein. As an approach to this problem, we are attempting to establish empirical relationships between the observed chemical shifts of Trp C^{γ} atoms and their environment, using the (crystalline) protein structure coordinates. For example, the torsion angles about α—β and β—γ (and other) bonds might be correlated with the chemical shift of C^{γ}. Other possible factors that might influence or dominate the chemical shift of C^{γ} include hydrogen bonding to the $N^{\epsilon 1}$ hydrogen, distance to the peptide carbonyl group, distance to the surface electrical double layer, and proximity of charged groups such as $-CO_2^-$. However, no clear picture has evolved yet.

A possible reason for this is that we have assumed the structure of the protein to be the same in solution as in the crystal. Fortunately, an answer to this possibility now appears feasible. High resolution ^{13}C nmr spectra can be obtained for solids by combining dilute-spin double resonance[12] with "magic-angle" sample spinning.[13–15] Dilute-spin double resonance has the effect of removing carbon-hydrogen dipolar interactions; "magic-angle" sample spinning removes line broadening effects due to static chemical shielding anisotropies, even at spinning frequencies that are less than the breadth of the powder pattern, expressed in frequency units.[15] Thus, it is possible, at least in principle, to obtain spectra of crystalline proteins with resolved single-carbon atom resonance lines. We hope it will soon be possible to compare chemical shifts of crystalline proteins directly with those found in solution, a comparison that may reveal structural differences.

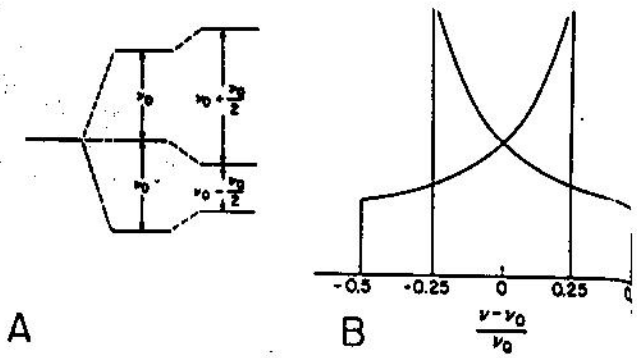

Figure 8 *a) Energy-level diagram for the spin I = 1 deuterium nucleus showing effect of first-order electric quadrupole interaction on Zeeman levels, assuming asymmetry parameter of $\eta = 0$ (axially symmetric electric field gradient). b) Line shapes for (+1⟶0) and (0⟶−1) transitions of ^2H nucleus in a C-D bond (I = 1, $\eta = 0$), showing spectral singularities (frequency separation $\nu_Q/2$) and distribution edges or steps (frequency separation ν_Q, where ν_Q is $3e^2qQ/2h$ or 255 kHz).*

Membrane structure by deuterium nmr

A second major interest in the authors' laboratory lies in the determination of biological membrane structure, using a combination of deuterium nmr, neutron-diffraction (with D. Worcester, University of London), and Raman-scattering (with R. Bansil, Boston University) measurements on specifically ^2H-labeled membrane systems. Deuterium nmr of ^2H-labeled model smectic liquid crystalline membranes and biological membranes was first reported some six or seven years ago using 8-MHz continuous-wave nmr instrumentation,[16,17] although studies of nematic phases were reported as early as 1965.[18] The deuterium nucleus has a spin I = 1 and thus possesses an electric quadrupole moment. The interaction between this electric quadrupole moment and the electric field gradient at the deuterium nucleus gives rise to a "quadrupole splitting" of the nuclear Zeeman energy levels so that separate transitions corresponding to +1⟷0 and 0⟷−1 may be observed (*Figure 8*). The splitting is dependent upon the orientation of the field gradient (C—D bond) with respect to H_0, and in a "rigid" crystal powder it gives rise to the line shape shown in Figure 8*b*. Molecular motions will tend to average out the splitting because of this angular dependence so that information about the motions may be extracted from the line shape and magnitude of the splitting.[16,19]

Unfortunately, ^2H-nmr studies, as well as having inherently low sensitivity, have the additional diffi-

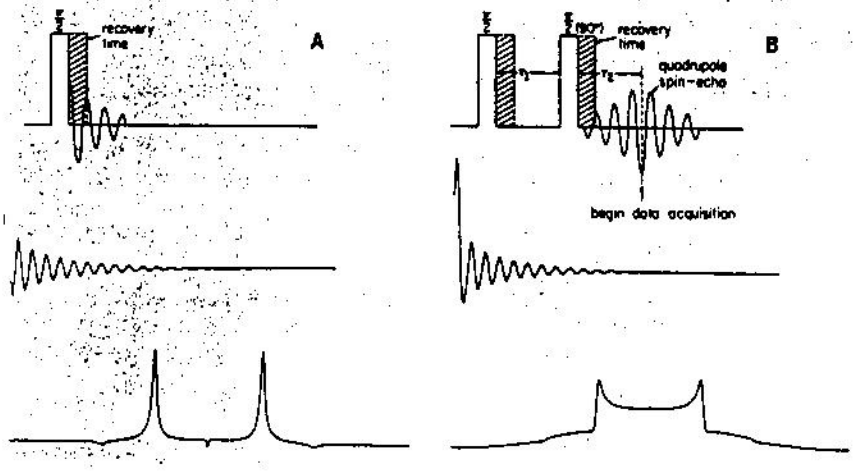

Figure 9 *Normal and quadrupole spin-echo ^2H Fourier transform nmr spectra of dimyristoylphosphatidylcholine labeled as CD_3 at the 6' position of the 2-chain. Spectra were obtained from about 50 mg of phospholipid dispersed in deuterium depleted water at 50°. a) Normal free-induction decay and Fourier transform spectrum, obtained using 90° pulse excitation. b) Free-induction decay and Fourier transform obtained by use of the quadrupole spin-echo pulse sequence.[20,21] An undistorted powder spectrum is obtained by use of the two-pulse sequence.*

culty that the ^2H-nmr powder pattern line shape may be 0.2 MHz in breadth. Conventional pulse Fourier transform experiments are therefore not feasible because finite spectrometer recovery times after a radiofrequency pulse (e.g., 50 μsec) cause unacceptable phase and amplitude distortions in the frequency domain spectra. Fortunately, however, a sequence of two 90° pulses gives essentially complete refocusing of the magnetization and provides a quadrupolar echo[20,21] (or solid echo). Data acquisition may thus be started at the echo maximum, eliminating phase and most amplitude errors, and resulting in significant improvements in signal-to-noise ratios. The pulse sequence and an example of its effectiveness are illustrated in *Figure 9*.

Using the quadrupole-echo pulse sequence, we have been investigating the structures of model and biological membranes. We are particularly interested in the interactions of cholesterol, and a variety of proteins and polypeptides, with the phospholipid molecule dimyristoylphosphatidylcholine (DMPC or lecithin) (see structure below) in smectic liquid crystalline model membrane systems. In addition, we are investigating the structures of intact biological membranes, in particular those from *Escherichia coli, Acholeplasma laidlawii* B (PG9), and the LM cell line of transformed mouse fibroblasts. Gains in spectrometer sensitivity in the last six or seven years now permit study of very small quantities (~200 μl) of even mammalian cell membranes that contain biosynthetically incorporated ^2H-labeled species.[22] With recent developments in techniques for incorporating fatty acids into cell membranes, for example by blocking fatty acid synthesis with avidin,[23] one may obtain up to 98% fatty acid homogeneity in a normal functioning cell membrane, so that realistic comparisons between model and biological membranes should now be possible.

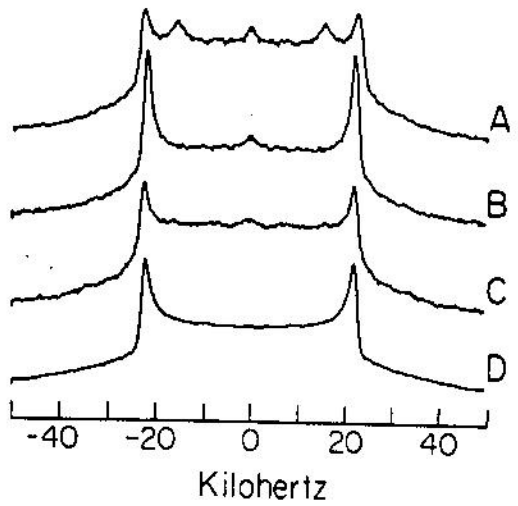

Figure 10 *Deuterium quadrupole-echo Fourier transform nmr spectra of 2(3,'3'-d_2) dimyristoylphosphatidylcholine -30 mole% cholesterol dispersions, at 30°C. a) Sample prepared by dissolving the lecithin and cholesterol in chloroform, then removing solvent at low temperatures. b) Sample prepared by dissolving lecithin and cholesterol in chloroform, then removing solvent by rotary evaporation at ~40°C). c) Spectrum of sample used in (a) after six freeze-thaw cycles in liquid nitrogen. d) Spectrum of sample prepared as in a but containing 2 wt% 1-myristoyl lysolecithin.*

Lecithin-cholesterol interactions

Figure 10 shows 34-MHz deuterium nmr spectra obtained on the lecithin/cholesterol system, where we have utilized a DMPC molecule containing a

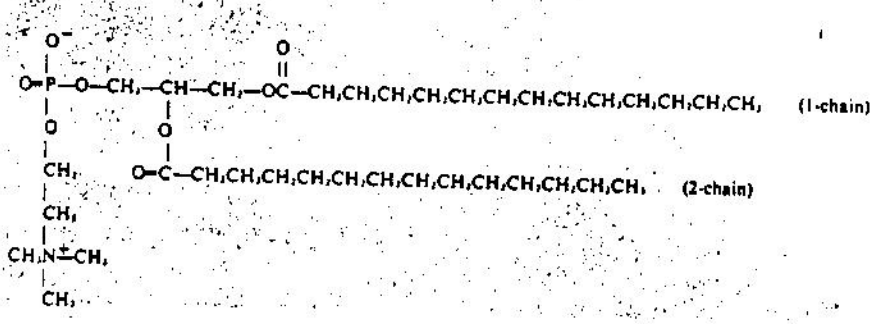

specifically enriched methylene group at position 3′ of the 2-chain. Cholesterol has the effect of increasing the order parameters of the CD segments of the hydrocarbon chain.[2,15] As shown in Figure 10, however, the nature of the sample is affected by the method of its preparation. Lecithin samples containing 30 mol% cholesterol give 2-component spectra (Figure 10*a*) when prepared by dissolving the dry components in chloroform, quenching to liquid nitrogen temperatures, and then rapidly evaporating the solvent in a lyophilizer. However, when the solvent is removed by rotary evaporation at temperatures above T_c, the gel-liquid crystal-phase transition temperature of the pure lecithin, the spectra have one component (Figure 10*b*).

The absence of residual solvent has been verified by ^{1}H nmr spectroscopy in benzene/methanol solutions. Furthermore, the 2-component samples give reproducible spectra even when the samples are incubated above T_c for several weeks (sample integrity being checked periodically by thin-layer chromatography), although mild sonication or passage through a series of freeze/thaw cycles converts the sample into the "normal" one-component system. These results suggest that incomplete mixing or a phase separation occurs in these samples during preparation. The effects we have seen, however, are most pronounced in lecithin labeled at the 3′ position of the 2-chain, and are removed on addition of small (~1%) quantities of impurity molecules such as lysolecithin. The observation of a metastable lecithin/cholesterol system may have biological implications, and may also help account for the wide range of lecithin/cholesterol "phase-diagrams" existing in the literature.

Results similar to those shown in Figure 10*b* have been obtained by us on DMPC's labeled at one of positions 3′, 4′, 6′, 8′, 10′, 12′, or 14′. In such spectra, the quadrupole splitting can be related to the projection of a C—C segment along the molecular axis, and the chain length can be determined as a sum of the projections. We have used this approach to determine the membrane thickness in the lecithin/cholesterol system, employing a variety of mathematical models similar to those previously used by Petersen and Chan[24] and by Seelig and Seelig.[19] Deuterium-labeled cholesterol was used as a probe of molecular tilt within the bilayer.[2] The chain lengths obtained are very insensitive to both the model and the tilt angle,[2] and are within experimental error the same as distance determinations made using high resolution neutron diffraction (*Table I*).[2] With this independent verification of the nmr method, one may now apply it to intact biological membranes, where sample orientation is impractical for neutron diffraction.

Protein-lipid interactions

Another application of ^2H nmr is to study the interaction between proteins (and polypeptides) and lipids in model membrane systems specifically labeled with deuterium. Conventional wisdom dictates that proteins be surrounded by a "halo" of rigid "boundary" lipid. Some evidence exists to support this view.[25,26] We find, however, that with the systems cytochrome b_3,[27] cytochrome oxidase,[28] bacteriophage fl coat protein,[29] gramicidin A,[29] mellitin,[30] and myelin proteolipid apoprotein (N-2),[16] there is a dynamic disordering of the terminal methyl region of the lipid bilayer above and below T_c, in the presence of the polypeptide chain. Typical results are shown in *Figure 11*. Time-scale differences between the EPR[31] and ^2H nmr experiments may account for the apparent lack of immobilized boundary lipid in the latter.

Determination of the structure of intact, functional biological membranes is the primary goal of our ^2H nmr, neutron, and Raman spectroscopic investigations. Earlier studies showed that large quantities of ^2H-labeled fatty acids could be incorporated into functional plasma membranes of the pleuropneumonia-like organism *Acholeplasma laidlawii* B.[32] More recently, ^2H-labeled choline head groups have been incorporated into a line of mammalian

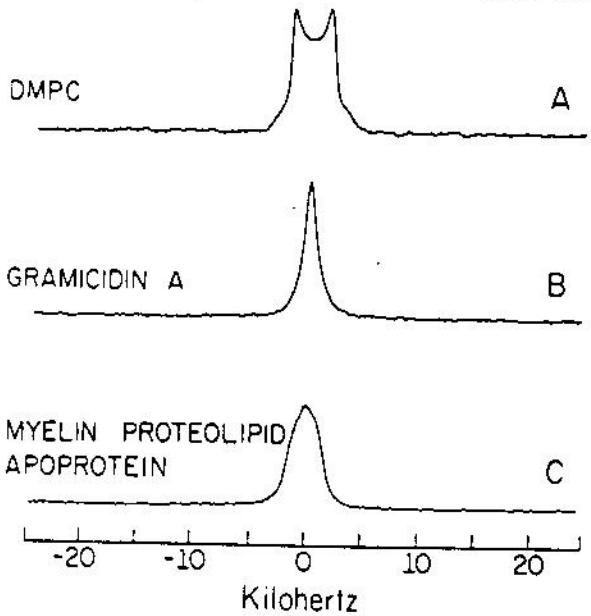

Figure 11 *Deuterium quadrupole-echo Fourier transform nmr spectra of 2(14', 14', 14'-d_3) dimyristoylphosphatidylcholine showing the dynamic disordering effect of a polypeptide and a protein on the terminal methyl region of the bilayer. a) Pure DMPC at 30°. b) DMPC bilayer containing 50 wt % gramicidin A. Sample was prepared by removing solvent (benzene 95%, MeOH 5%) by lyophilization.[29] c) DMPC bilayer containing 67 wt % beef brain proteolipid apoprotein.[16]*

Table 1

Comparison of lecithin/cholesterol[a] bilayer structures determined by magnetic resonance spectroscopy and high resolution neutron diffraction

	$l = \sum_{l=2}^{l=6} \langle I_l \rangle$[b]	$l = \sum_{l=6}^{l=12} \langle I_l \rangle$[c]	L_z[d] (Å)	L_b[e] (Å)	L_{12}[f] (Å)
nmr	4.5	6.8	30.	21.	8.
Neutron diffraction[g]	4.4	7.5	33.	24.	9.

[a] 30 mol % cholesterol, 23°C.

[b] Distance from C-2′ to C-6′ in the 2-chain of DMPC.

[c] Distance from C-6′ to C-12′ in the 2-chain of DMPC.

[d] Transmembrane thickness at C-2′ of the 2-chain of DMPC.

[e] Transmembrane thickness at C-6′ of the 2-chain of DMPC.

[f] Transmembrane thickness at C-12′ of the 2-chain of DMPC.

[g] Neutron data were obtained on oriented multilayer domains at 86% relative humidity (D.L. Worcester, M. Meadows, D. Rice, and E. Oldfield, unpublished results). The estimated error is about ± 1.0 Å.

cells in tissue culture.[32] For the simpler microorganisms like *A. laidlawii* and *Escherichia coli* it appears that significant quantities of membrane lipids may exist in the rigid crystalline gel phase,[31] although quantitation of the amount of this phase has always been difficult.[32,33]

In current work,[34] we have found that it is relatively simple to quantitate the phase composition accurately with the deuterium quadrupole-echo pulse experiment when using specifically labeled lipids biosynthetically incorporated into an *E. coli* fatty acid auxotroph. *Figure 12* shows typical results obtained using the auxotroph L48-2, generously provided by Professor David Silbert, into which has been biosynthetically incorporated terminal methyl ^{2}H-labeled hexadecanoic acid. Deuterium quadrupole-echo Fourier transform nmr spectra observed at 3 and 40° are shown in Figures 12*a* and 12*c*, and the corresponding spectral simulations are given in Figures 12*b* and 12*d*. It is estimated that the percentage of solid lipid may be determined to within ~5%.[34]

The results outlined in this article represent the current state-of-the-art in sensitivity for studies of proteins by ^{13}C nmr and of membranes by ^{2}H nmr spectroscopy. However, it should be noted that the acquisition of spectra with high signal-to-noise ratio is still exceedingly time-consuming. Further developments in magnet technology in the direction of increased fields (and decreased costs) are highly desirable. For deuterium, the low gyromagnetic ratio means that its Larmor frequency at higher fields would be in a region that provides few radiofrequency-circuitry difficulties. Thus, fields in excess of 23.5 T (154 MHz for deuterium, 1000 MHz for protons) could immediately reduce data acquisition times by more than an order of magnitude for deuterium. The situation as regards protons at such high fields is, of course, less clear.

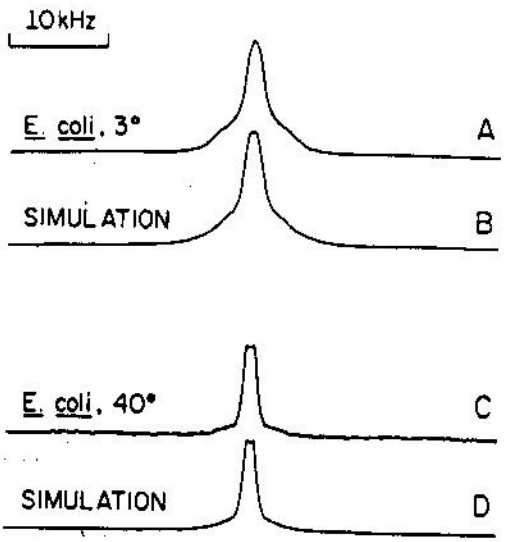

Figure 12 *Deuterium quadrupole-echo Fourier transform nmr spectra of E. coli cell membranes containing biosynthetically incorporated 16,16,16-d$_3$ hexadecanoic acid: a) at 3°, b) spectral simulation of 3° spectrum, c) at 40°, d) spectral simulation of 40° spectrum. Both spectra are simulated by two overlapping ^{2}H powder patterns.[34] The 3° spectrum contains 54% solid and the 40° spectrum 33% solid phase lipid.*

References

1. OLDFIELD, E. and MEADOWS, M., *J. Magn. Res.*, in press (1978).
2. OLDFIELD, E., MEADOWS, M., RICE, D., and JACOBS, R., *Biochemistry 17*, 2727, (1978).
3. DODDRELL, D., GLUSHKO, V., and ALLERHAND, A., *J. Chem. Phys. 56*, 3683, (1972).
4. OLDFIELD, E., NORTON, R.S., and ALLERHAND, A., *J. Biol. Chem. 250*, 6368 (1975).
5. ALLERHAND, A., CHILDERS, R.F., GOODMAN, R.A., OLDFIELD, E., and YSERN, X., *Amer. Lab. 4*, 19 (1972).
6. ABRAGAM, A., *The Principles of Nuclear Magnetism* (Clarendon Press, Oxford, 1961).
7. HOULT, D.I. and RICHARDS, R.E., *J. Magn. Res. 24*, 71 (1976).
8. CARR, H.Y. and PURCELL, E.M., *Phys. Rev. 94*, 630 (1954).
9. OLDFIELD, E. and SKARJUNE, R.P., *J. Magn. Res.* (in press, 1978).
10. ALLERHAND, A., CHILDERS, R.F., and OLDFIELD, E., *Biochemistry 12*, 1335 (1973).
11. CAMPBELL, I.D., DOBSON, C.M., WILLIAMS, R.J.P., and XAVIER, A., *J. Magn. Res. 11*, 172 (1973).
12. PINES, A., GIBBY, M.G., and WAUGH, J.S., *J. Chem. Phys. 59*, 569 (1973).
13. ANDREW, E.R., BRADBURY, A., and EADES, R.G., *Nature 182*, 1659 (1958).
14. LOWE, I., *Phys. Rev. Letts. 2*, 285 (1959).
15. LIPPMAA, E., ALLA, M., and TUHERM, T., *Proceedings of the XIXth Congress Ampere, Heidelberg*, 113 (1976).
16. OLDFIELD, E., CHAPMAN, D., and DERBYSHIRE, W., *FEBS Lett. 16*, 102 (1971).
17. OLDFIELD, E., CHAPMAN, D., and DERBYSHIRE, W., *Chem. Phys. Lipids 9*, 69 (1972).
18. ROWELL, J.C., PHILLIPS, W.D., MELBY, L.R., and PANAR, M., *J. Chem. Phys. 43*, 3442 (1965).
19. SEELIG, A. and SEELIG, J., *Biochemistry 13*, 4839 (1974).
20. SOLOMON, I., *Phys. Rev. 110*, 61 (1958).
21. DAVIS, J.H., JEFFREY, K.R., BLOOM, M., VALIC, M.I., and HIGGS, T.P., *Chem. Phys. Letts. 42*, 390 (1976).
22. OLDFIELD, E., MEADOWS, M., and GLASER, M., *J. Biol. Chem. 251*, 6147 (1976).
23. SILVIUS, J.R. and MC ELHANEY, R.N., *Nature 272*, 645 (1978).
24. PETERSEN, N.O. and CHAN, S.I., *Biochemistry 16*, 2657 (1977).
25. JOST, P.C., GRIFFITH, O.H., CAPALDI, R.A., and VANDERKOOI, G., *Proc. Natl. Acad. Sci. U.S.A. 70*, 480 (1973).
26. DAHLQUIST, F.W., MUCHMORE, D.C., DAVIS, J.H., and BLOOM, M., *Proc. Natl. Acad. Sci. U.S.A. 74*, 5435 (1977).
27. GILMORE, R., GLASER, M., and OLDFIELD, E., unpublished results.
28. KANG, S.Y., GUTOWSKY, H.S., KING, T.E., and OLDFIELD, E., unpublished results.
29. RICE, D. and OLDFIELD, E., unpublished results.
30. MEADOWS, M. and OLDFIELD, E., unpublished results.
31. OLDFIELD, E., *Science 180*, 982 (1973).
32. ENGELMAN, D.M., *J. Mol. Biol. 58*, 153 (1971).
33. ESFAHANI, M., LIMBRICK, A.R., KNUTTON, S., OKA, T., and WAKIL, S., *Proc. Natl. Acad. Sci. U.S.A. 68*, 3180 (1971).
34. KANG, S.Y., GUTOWSKY, H.S., and OLDFIELD, E., unpublished results.